

MCRAGE: Synthetic Healthcare Data for Fairness

Keira Behal ^{*}, Jiayi Chen ^{*}, Caleb Fikes [†], and Sophia Xiao ^{*}

Project advisor: Yuanzhe Xi

Abstract. In the field of healthcare, electronic health records (EHR) serve as crucial training data for developing machine learning models for diagnosis, treatment, and the management of healthcare resources. However, medical datasets are often imbalanced in terms of sensitive attributes such as race/ethnicity, gender, and age. Machine learning models trained on class-imbalanced EHR datasets perform significantly worse in deployment for individuals of the minority classes compared to those from majority classes, which may lead to inequitable healthcare outcomes for minority groups. To address this challenge, we propose Minority Class Rebalancing through Augmentation by Generative modeling (MCRAGE), a novel approach to augment imbalanced datasets using samples generated by a deep generative model. The MCRAGE process involves training a Conditional Denoising Diffusion Probabilistic Model (CDDPM) capable of generating high-quality synthetic EHR samples from underrepresented classes. We use this synthetic data to augment the existing imbalanced dataset, resulting in a more balanced distribution across all classes, which can be used to train less biased downstream models. We measure the performance of MCRAGE versus alternative approaches using Accuracy, F1 score and AUROC of these downstream models. We provide theoretical justification for our method in terms of recent convergence results for DDPMs.

Key words. synthetic electronic health records, conditional denoising diffusion probabilistic model, healthcare AI, tabular data, fairness, synthetic data

1. Introduction. In recent years, reliance on machine learning algorithms to facilitate decision-making processes across various industries has grown. In healthcare, clinicians may use machine learning models to predict disease progression, improve diagnosis accuracy, and optimize treatment plans [25]. However, machine learning approaches may perpetuate existing societal biases, leading to inequitable treatment for minority groups, because machine learning models trained on imbalanced datasets may replicate and thus amplify these biases [5].

These issues are of utmost concern in healthcare applications where fair and equitable treatment is of critical importance. Ideally, a well-engineered machine learning model should be fair, optimizing health outcomes to provide high-quality, individualized care to all patients, regardless of their demographic characteristics [23]. Unfortunately, healthcare datasets are often imbalanced across several dimensions, including race, socioeconomic status, age, and gender [15, 8]. As a result, models trained on these datasets struggle to generalize effectively to individuals who are not well represented in the data [28].

EHRs are a valuable data source in healthcare, providing a comprehensive snapshot of a patient’s health history, including diagnoses, treatments, and demographic information [26]. Certain demographic groups, such as specific racial or ethnic minorities, are often underrepresented in the EHR datasets [33]. This imbalance might lead to inequitable health outcomes,

^{*}Department of Mathematics, Emory University, Atlanta, GA 30322 (keira.behal@emory.edu,jiayi.chen@emory.edu,sxxiao@emory.edu)

[†]Department of Mathematics, Rice University, Houston, TX 77005 & Department of Mathematics, Emory University, Atlanta, GA 30322 (cfikes@emory.edu)

39 in which minority groups are more likely to receive less accurate diagnoses or treatment rec-
40 ommendations due to their lack of representation in the training data [24]. Consequently,
41 addressing the challenge of dataset imbalance is vital in the pursuit of creating machine learn-
42 ing applications that are equitable and beneficial for all patient groups within healthcare.

43 In this paper, we mitigate imbalance-induced bias in machine learning models trained
44 on EHR datasets via an innovative approach, MCRAGE. We demonstrate the utility of this
45 method to rectify the imbalance found in medical datasets by supplementing them with sam-
46 ples synthesized by a deep generative model. Central to MCRAGE is the utilization of a
47 Conditional Denoising Diffusion Probabilistic Model, which has been specifically trained to
48 generate high-fidelity synthetic EHR samples from underrepresented classes [9]. By integrat-
49 ing this synthetic data into the original, imbalanced dataset, we aim to approximate a more
50 equitable distribution across all classes.

51 **Our contributions:**

- 52 • We propose a novel framework, MCRAGE, for applying a CDDPM or other generative
53 model to generate synthetic samples of minority class individuals to rebalance an
54 imbalanced dataset as a preprocessing step to the enhance the fairness of a downstream
55 classifier.
- 56 • We show that the synthetically generated minority class data increases classifier accu-
57 racy and fairness when used to supplement an imbalanced dataset.
- 58 • We demonstrate a significant improvement over established methods (i.e. SMOTE) in
59 terms of fairness, and discuss regimes in which such improvements will likely justify
60 associated computational cost.
- 61 • We motivate future theoretical work relating to the convergence of CDDPMs based
62 on that for DDPMs and empirical observation of convergent behavior.

63 **2. Related Works.**

64 **2.1. Methods for Dealing with Imbalanced Datasets.** Generally, there are two kinds of
65 methods for dealing with imbalanced datasets: data-level methods, which involve modifying
66 the dataset by resampling or augmenting the dataset as a preprocessing step, and classifier-
67 level methods, which involve modifications to the training objective or inference [12]. Since
68 data-level techniques are implemented as a preprocessing step, they are model-agnostic and
69 generally more flexible [10]. Therefore, in this paper, we focus on data-level solutions to the
70 class imbalance problem.

71 **2.2. Resampling and Undersampling Methods.** A variety of techniques have been pro-
72 posed with the goal of rebalancing data [2]. The most common approach for resampling is
73 SMOTE and SMOTE-based algorithms that synthesize new minority class samples via linear
74 interpolation of existing samples to augment the dataset [4]. However, oversampling meth-
75 ods may introduce flawed correlations and dependencies between samples, resulting in limited
76 data variability [14]. Moreover, SMOTE-based methods may fail to effectively handle multi-
77 modal data, datasets with high intra-class overlap, or noise [10]. As a result, SMOTE is not
78 sufficiently sophisticated to be a general solution to this problem.

79 Undersampling methods have not been widely studied [10] since random undersampling
80 can lead to the loss of potentially useful information [13]. This is especially damaging when

81 dealing with a dataset with a significant class imbalance, as undersampling requires discarding
82 a large portion of the majority class data, potentially meaning the loss of important patterns
83 and details that the model could learn from [10]. Moreover, due to chance, random undersam-
84 pling may also introduce bias and result in the under-representation of certain characteristics
85 of the majority class [19].

86 **2.3. Synthetic Data Generation for EHRs.** As generative models become capable of
87 producing synthetic samples indistinguishable from real ones, numerous studies have inves-
88 tigated the potential application of these synthetic samples in the training of other models.
89 In particular, realistic EHR data can be generated for "imaginary" individuals who need not
90 be anonymized. Synthetic EHR data already promises to revolutionize the field of health-
91 care AI by offering data privacy and missing value-imputation solutions, and our method
92 further expands the utility of such methods in applications for equitable performance across
93 intersectional demographic groups.

94 One impactful study involved defining the concept of synthetic data and demonstrating
95 the practical application of the ATEN framework, a tool for validating realism in synthetic
96 data generation [22]. In another study, deep learning harnessed the encoder-decoder model,
97 a tool often found in machine translation systems [20]. This model facilitated the creation of
98 synthetic chief complaints based on discrete variables found in electronic health records.

99 However, applying these datasets presents its own challenges. The crucial need to preserve
100 the privacy of sensitive information has always been a substantial obstacle. To address this,
101 several researchers proposed the use of Generative Adversarial Networks to create synthetic,
102 heterogeneous EHRs as a replacement for existing datasets [7]. A separate study introduced
103 the Sequentially Coupled Generative Adversarial Network (SC-GAN), a network developed
104 to focus on the continuous generation of patient state and medication dosage data, furthering
105 the pursuit of patient-centric data [31].

106 In the most recent advancement, a study proposed a Hierarchical Autoregressive Language
107 model (HALO) [30]. This model, designed to generate high-dimensional longitudinal EHRs,
108 stands out for its ability to preserve the statistical properties of real EHRs, which, in turn,
109 allows for the training of highly accurate machine learning models without raising any privacy
110 concerns.

111 All these advancements collectively emphasize the significant strides made in the gener-
112 ation and utilization of synthetic data, highlighting its immense potential in the healthcare
113 industry. Our work extends previous work in synthetic data generation by focusing on a regime
114 of particular importance – a classifier whose original training set is necessarily imbalanced.

115 **2.4. Denoising Diffusion Probabilistic Models.** It is critical in a healthcare setting that a
116 diagnostic model be trained on the highest quality data, as even a few low-quality or badly out-
117 of-distribution samples could cause serious medical consequences. This requirement of reliable,
118 specific, and realistic samples leads us to choose the DDPM as our generative model due to its
119 recent success in generating high-fidelity images [11]. Diffusion models are characterized by
120 a forward process, which systematically incorporates noise into the initial data sample, and
121 a reverse process, which methodically removes the noise added in the forward process [17].
122 In the reverse process, sampling begins at the T th noise level, \mathbf{x}_T , and each subsequent step
123 yields incrementally denoised samples, i.e., $\mathbf{x}_{t-1}, \mathbf{x}_{t-2}, \dots, \mathbf{x}_0$. Essentially, the diffusion model

124 learns how to obtain the “denoised” version from \mathbf{x}_{t-1} to \mathbf{x}_t .

125 Diffusion models outperform other generative modeling classes [16] due to several unique
126 advantages. In contrast to GANs, diffusion models eliminate the need for adversarial training,
127 a process known for its susceptibility to mode collapse and difficulties in effective implementa-
128 tion [27]. Furthermore, diffusion models may be implemented with many kinds of architectures
129 [6]. Diffusion models are also able to capture the diversity and intricate distributions of com-
130 plicated datasets; for example, in the fields of image and speech synthesis, diffusion-based
131 models can deliver high-quality, diverse samples that supersede the output of their GAN
132 equivalents [1]. In fact, DDPMs produce superior-quality images relative to other generative
133 models such as GANs and VAEs, with impressive results documented on the CIFAR10 and
134 256x256 LSUN benchmarks [16].

135 Ho et al’s groundbreaking development of DDPMs offered a specific parameterization of
136 the diffusion model to simplify the training process, utilizing a loss function similar to score
137 matching to minimize the mean-squared error between the actual and predicted noise [16].
138 This work highlights that the sampling process can be interpreted as being analogous to
139 Langevin dynamics, connecting the DDPMs to the score-based generative models [29].

140 DDPMs may also be used to synthesize high-quality structured data. Specifically, tabular
141 data, a prevalent and critical data format in real-world applications, poses unique challenges
142 due to its inherent heterogeneity, with data points often constituted by a mixture of continuous
143 and discrete features. A recent development in this area is the introduction of TabDDPM, a
144 model capable of handling any feature type present in tabular datasets [18]. Demonstrating
145 superior performance over existing GAN/VAE alternatives, this model proves applicable in
146 privacy-sensitive settings, such as healthcare, where direct data point sharing is infeasible [18].

147 **2.5. CDDPM.** Because of the stochasticity inherent to the generative process in the
148 DDPM, users lack control over the class of images generated. This randomness could po-
149 tentially result in generated images that are not aligned with desired categories or classes,
150 thereby posing a challenge when specific classes of images are required; to mitigate this issue,
151 researchers introduced an approach known as “classifier-free guidance” [17]. Instead of utiliz-
152 ing a classifier to direct the generation process towards desired classes, this method proposes
153 a simultaneous training of two diffusion models, one conditional and one unconditional.

154 The conditional diffusion model is trained with labeled data, while the unconditional diffu-
155 sion model is trained with unlabeled data, thus generating samples without any class-specific
156 guidance. After the training process, context embeddings (representing class information in
157 vector format for guiding the generation process) and timestep embeddings (capturing the
158 evolution of the generative process over time) are used to combine score estimates from both
159 models [17]. Thus this method provides a nuanced way of guiding the generative process in a
160 class-aware manner, without the direct involvement of an additional classifier model.

161 This can be beneficial in scenarios where classifier-based guidance is not desirable or fea-
162 sible. This section addresses the mathematical formulation of the Conditional DDPM (CD-
163 DPM) model used in this study. Note that these formulas are compatible with the definitions
164 given in [3].

165 **Forward Process.** The forward process consists of a Markov process which iteratively
 166 perturbs data with random noise until the data diffuses to an isotropic Gaussian:

$$167 \quad q(\mathbf{x}_1, \dots, \mathbf{x}_T | \mathbf{x}_0) = \prod_{t=1}^T q(\mathbf{x}_t | \mathbf{x}_{t-1}).$$

168 Using the Gaussian transition kernel

$$169 \quad q(\mathbf{x}_t | \mathbf{x}_{t-1}) = \mathcal{N}(\mathbf{x}_t; \sqrt{1 - \beta_t} \mathbf{x}_{t-1}, \beta_t \mathbf{I}),$$

170 we can find a closed-form solution to sample \mathbf{x}_t directly from \mathbf{x}_0 using special properties of
 171 the Gaussian distribution and Markov processes,

$$172 \quad q(\mathbf{x}_t | \mathbf{x}_0) = \mathcal{N}(\mathbf{x}_t; \sqrt{\bar{\alpha}_t} \mathbf{x}_0, (1 - \bar{\alpha}_t) \mathbf{I}),$$

173 where β_t is assigned by a schedule (we use a linear schedule in our experiments), $\alpha_t := 1 - \beta_t$
 174 and $\bar{\alpha}_t := \prod_{s=1}^t \alpha_s$. When $\bar{\alpha}_T \approx 0$, i.e., betas are small, \mathbf{x}_T is approximately Gaussian, so

$$175 \quad q(\mathbf{x}_T) := \int q(\mathbf{x}_T | \mathbf{x}_0) q(\mathbf{x}_0) d\mathbf{x}_0 \approx \mathcal{N}(\mathbf{x}_T; 0, I).$$

176 **Reverse Process.** In order to generate new data samples, CDDPMs must learn the reverse
 177 Markov process by iteratively denoising from an isotropic Gaussian. At each timestep t , we
 178 parameterize the reverse process for CDDPM as:

$$179 \quad p_\theta(\mathbf{x}_{t-1} | \mathbf{x}_t, \mathbf{c}) = \mathcal{N}(\mathbf{x}_{t-1}; \mu_\theta(\mathbf{x}_t, t, \mathbf{c}), \Sigma_\theta(\mathbf{x}_t, t, \mathbf{c})),$$

180 where \mathbf{c} is the class label embedding, as in [17] and the mean and variance are parameterized
 181 in this model by:

$$182 \quad \mu_\theta(\mathbf{x}_t, t, \mathbf{c}) = \frac{1}{\sqrt{\alpha_t}} \left(\mathbf{x}_t - \frac{\beta_t}{\sqrt{1 - \alpha_t}} \boldsymbol{\epsilon}_\theta(\mathbf{x}_t, t, \mathbf{c}) \right),$$

$$183 \quad \Sigma_\theta(\mathbf{x}_t, t, \mathbf{c}) = \frac{1 - \alpha_t}{1 - \alpha_{t-1}} \beta_t \mathbf{I},$$

185 where $\boldsymbol{\epsilon}_\theta$ is a neural net trained to predict ϵ given $(\mathbf{x}_t, t, \mathbf{c})$, so that synthetic samples can be
 186 generated by drawing from $p_\theta(\mathbf{x}_{\tau-1} | \mathbf{x}_\tau, \mathbf{c})$ sequentially for $\tau \in \{T, \dots, 0\}$. The loss function
 187 used for training this model is derived by the variational bound on negative log likelihood:

$$188 \quad \mathbb{E}[-\log p_\theta(\mathbf{x}_0, \mathbf{c})] \leq \mathbb{E}_q \left[\log \frac{p_\theta(\mathbf{x}_{0:T}, \mathbf{c})}{q(\mathbf{x}_{1:T} | \mathbf{x}_0)} \right] =: L.$$

189 As proposed by Ho et al., we reweight L to obtain a simplified loss function [16]:

$$190 \quad L_{simple} = \|\boldsymbol{\epsilon} - \boldsymbol{\epsilon}_\theta(\sqrt{\bar{\alpha}} \mathbf{x}_0 + \sqrt{1 - \bar{\alpha}} \boldsymbol{\epsilon}, t, \mathbf{c})\|^2.$$

191 This mathematical formulation underpins the CDDPM model’s forward and reverse pro-
 192 cesses, providing a foundation for class-aware generation and control.

193 **3. Methods.** Prior to recent developments in generative models, imbalanced distributions
 194 of key demographic traits such as race, sex, age, and socioeconomic status in EHR data seemed
 195 to be an inescapable obstacle in creating automated healthcare systems. Motivated by the
 196 constant presence of such imbalances and their detrimental effect on minority outcomes, we
 197 desire a model-agnostic method of improving classifier accuracy for minority groups without
 198 compromising overall performance. We believe generative models, specifically DDPMs, hold
 199 the key to this capability.

200 In an optimal case, a researcher intending to train a classifier using imbalanced EHR
 201 data could simply collect or ask for new samples specifically from the minority class. Given
 202 enough of these samples, they might collect a stratified sample, one with an equal number of
 203 individuals in each class. If the data has multiple demographic features, they may even collect
 204 an intersectionally-stratified sample. Such a classifier would have more equitable predictions,
 205 as each epoch of training would include the same number of samples from each group, and
 206 thus the classifier would implicitly weight each class’s outcomes as equally important.

207 In practice, collection of new data is often cost-prohibitive or impossible, however re-
 208 cent work guarantees convergence of the distribution of DDPM methods [3]. The result is
 209 contingent on the following assumptions:

- 210 1. the true distribution of the data has compact support containing 0 (in particular if
 211 the data are contained in some manifold \mathcal{M} , then $\text{diam}(\mathcal{M})$ is bounded.),
- 212 2. the schedule $t \mapsto \beta_t$ is continuous, non-decreasing, and $\exists \bar{\beta} : \forall t \in [0, T], 1/\bar{\beta} \leq \beta_t \leq \bar{\beta}$
 213 (for our purposes, take $\bar{\beta} = \beta_T$),
- 214 3. there is some estimate score function \mathbf{s} such that $\exists M \geq 0$ such that $\forall t \in [0, T],$
 215 $\mathbf{x}_t \in \text{supp}(\mathcal{M})$

$$216 \quad \|\mathbf{s}(t, \mathbf{x}_t) - \nabla \log(p_t(\mathbf{x}_t))\| \leq M \left(\frac{1 + \|\mathbf{x}_t\|}{\sigma_t^2} \right),$$

217 where $\sigma_t^2 = 1 - \exp(-2 \sum_{s=0}^t \beta_s)$, and

- 218 4. using unit stepsizes $\gamma_\kappa = 1 \quad \forall \kappa$, by applying the transformation $\epsilon = 1/32, t = t'/32,$
 219 $T = T'/32$ (where T' is the number of stepsizes in our unit stepsize implementation),
 220 then $\exists \delta : \forall t \in \{1, \dots, T\}, \beta_t \leq \frac{2^{-6}\delta}{1+2^{-4}\beta_0}$

221 The theorem states that under these assumptions, and for a sufficiently large T' that

$$222 \quad \frac{T'}{32} = T \geq 2\bar{\beta}(1 + \log(1 + \text{diam}(\mathcal{M}))),$$

223 and some hyperparameters $M, \delta \leq \frac{1}{32}$, there is a bound on the Wasserstein 1-distance between
 224 the data distribution and the sampling distribution of a DDPM. The bound in our case is, for
 225 some $D_0 \in \mathbb{R}$,

$$226 \quad \mathbf{W}_1(\mathcal{L}(Y_k), \pi) \leq D_0 \left(2^{10} \exp(2^5 \text{diam}(\mathcal{M})^2) (M + \delta^{1/2}) + \exp \left(2^5 \text{diam}(\mathcal{M})^2 - \frac{T}{\bar{\beta}} \right) + 1 \right),$$

$$227 \quad D_0 = D(1 + \bar{\beta})^7 (1 + d + \text{diam}(\mathcal{M})^4) (1 + \log(1 + \text{diam}(\mathcal{M}))).$$

228 As discussed in that paper, these assumptions on the score function are mild enough to be
 229 frequently met by real world datasets such as EHRs. Crucially, the convergence bound gives
 230 us a lower limit for T , which we use to set this hyperparameter in our implementation.

231 Although such a convergence result has not yet been proven for the convergence of a
 232 conditional DDPM, our numerical experiments suggests that such a theorem is likely true.
 233 Theoretically, such a statement would guarantee that under some conditions, synthetic samples
 234 of a given class generated by a CDDPM will approximate legitimate samples of that class well.
 235 Thus, in any case where the given minority data is enough to sufficiently train the CDDPM,
 236 further samples needed for training a downstream model can be approximated by training and
 237 drawing from that model. The capability to synthetically draw new minority-class samples
 238 quickly and cheaply from a distribution that may otherwise be costly or inaccessible to draw
 239 from enables exciting new solutions for imbalanced EHR data.

240 In order to standardize the synthetic data rebalancing process, we propose the MCAGE
 241 process. This algorithm first calculates a bijection from a Cartesian product of indices rep-
 242 resenting several demographic attributes and one diagnosis to a single index representing
 243 particular intersectional groups. This process is denoted as ϕ in the pseudocode. Next, the
 244 process identifies the most prevalent intersectional group and finds the number of samples
 245 missing from each other group relative to the majority. Next, a CDDPM or similar condi-
 246 tioned generative model is trained on the serialized data. In the final step, we generate new
 247 samples from all except the majority class, and append them to our training data, which is
 248 then used to train a classifier.

Algorithm 3.1 MCAGE

Require: s_1, \dots, s_L are categorical variables representing demographic attributes, (χ_0, Y_0)
 are observed data-diagnosis pairs.

- 1: $\bar{s} \leftarrow Y_0 \times \prod_{\ell}^L s_{\ell}$. ▷ Cartesian Product.
 - 2: $s_0 \leftarrow \phi(\bar{s})$.
 - 3: $K \leftarrow \max(s_0)$. ▷ the number of unique intersectional categories.
 - 4: $\hat{\pi}_k \leftarrow \mathbb{P}(s = k)$ for all $k \in \{1, \dots, K\}$.
 - 5: $k^* \leftarrow \operatorname{argmax}_k \hat{\pi}_k$.
 - 6: $T' \leftarrow \lceil 2^6 \hat{\beta}(1 + \log(1 + \operatorname{diam}(\chi_0))) \rceil$. ▷ using the transformation $T' = 32T$ from above.
 - 7: Train CDDPM $p_{\theta}(\mathbf{x}_0 | \mathbf{x}_{T'}, \mathbf{c})$ on data (χ_0, s_0) .
 - 8: **for** $k \in \{1, \dots, K\}$ **do**
 - 9: $\chi_k \leftarrow n(\hat{\pi}_{k^*} - \hat{\pi}_k)$ samples drawn from $p_{\theta}(\mathbf{x}_0 | \mathbf{x}_{T'}, \mathbf{c} = k)$.
 - 10: $(Y_k, S_k^1, \dots, S_k^L) \leftarrow \phi^{-1}(k)$.
 - 11: **end for**
 - 12: **return** $(\{\chi_0, \dots, \chi_K\}, \{(s_1, \dots, s_K), (S_1^1, \dots, S_1^L), \dots, (S_K^1, \dots, S_K^L)\}, \{Y_0, \dots, Y_K\})$.
-

249 The MCAGE process is both intuitive and theoretically justified. The algorithm re-
 250 sults in a synthetically rebalanced training set where each intersectional group is equally
 251 represented. By generating an artificially stratified sample, the process enforces the fairness
 252 conditions of statistical parity and balanced accuracy. In practice, this ensures that the distri-
 253 bution of outcomes or predictions across different subgroups is similar, and that the classifier’s
 254 performance is evaluated fairly for each subgroup, accounting for class imbalances. Each of
 255 these properties is desirable as an indicator of equitable performance across all intersectional
 256 groups.

257 **3.0.1. MCRAGE Specifics.** The notation of the MCRAGE Algorithm may be daunting,
 258 but the algorithm is simply motivated. \bar{s} can be thought of as a collection of “buckets” of
 259 data who would ideally be equally full. As explained below, ϕ essentially maps \bar{s} to a list of
 260 buckets with a single index. The next three steps subsequently calculate K , $\hat{\pi}_k$, and k^* , which
 261 are the number of buckets, relative proportion in each bucket, and index of the “majority”
 262 bucket, respectively. The remainder of the algorithm simply trains a CDDPM on all available
 263 data, and samples enough samples from each category so that all buckets are as full as the
 264 majority bucket k^* .

265 A key step in the MCRAGE algorithm is the generation of an index mapping – an invertible
 266 map from an L-tuple of categorical variables to a single categorical variable with many levels
 267 representing each intersectional group. In the algorithm presented in this paper, we denote
 268 this map as $\phi(u_1, \dots, u_L)$.

$$269 \quad \phi(u_1, \dots, u_L) = \sum_{i=1}^L u_i \prod_{j=0}^{i-1} K_j,$$

270 Where K_j is the number of distinct values taken by u_j . The inverse of this map can be
 271 calculated as follows:

$$272 \quad (\phi^{-1}(y))_j = \frac{y \bmod K_j - y \bmod K_{j-1}}{\prod_{\ell=0}^{j-1} K_\ell}.$$

273 The linear combinations that define ϕ are inspired by the concept of iteratively “stacking”
 274 a discrete lattice of intersectional groups to eventually index in one dimension. To prove that
 275 ϕ and ϕ^{-1} are inverses, we need to show two conditions:

- 276 1. $\phi^{-1}(\phi(u_1, \dots, u_L)) = (u_1, \dots, u_L)$
- 277 2. $\phi(\phi^{-1}(y)) = y$

278 We will begin with the first condition:

$$\begin{aligned}
 279 \quad \phi^{-1}(\phi(u_1, \dots, u_L)) &= \phi^{-1} \left(\sum_{i=1}^L u_i \prod_{j=0}^{i-1} K_j \right) \\
 280 \quad &= \left(\frac{\left(\sum_{i=1}^L u_i \prod_{j=0}^{i-1} K_j \right) \bmod K_1 - \left(\sum_{i=1}^L u_i \prod_{j=0}^{i-1} K_j \right) \bmod 1}{\prod_{\ell=0}^0 K_\ell}, \dots, \right. \\
 281 \quad &\quad \left. \frac{\left(\sum_{i=1}^L u_i \prod_{j=0}^{i-1} K_j \right) \bmod K_L - \left(\sum_{i=1}^L u_i \prod_{j=0}^{i-1} K_j \right) \bmod K_{L-1}}{\prod_{\ell=0}^{L-1} K_\ell} \right) \\
 282 \quad &= (u_1, \dots, u_L).
 \end{aligned}$$

284 Now, we will move on to the second condition:

$$\begin{aligned}
285 \quad \phi(\phi^{-1}(y)) &= \phi \left(\frac{y \bmod K_1 - y \bmod 0}{\prod_{\ell=0}^0 K_\ell}, \dots, \frac{y \bmod K_L - y \bmod K_{L-1}}{\prod_{\ell=0}^{L-1} K_\ell} \right) \\
286 \quad &= \left(\sum_{i=1}^L \frac{y \bmod K_i - y \bmod K_{i-1}}{\prod_{j=0}^{i-1} K_j} \right) \\
287 \quad &= \sum_{i=1}^L \frac{y \bmod K_i - y \bmod K_{i-1}}{\prod_{j=0}^{i-1} K_j} \\
288 \quad &= y.
\end{aligned}$$

290 This concludes our proof that the index mapping function ϕ in the MCRAGE algorithm is a
291 bijection as specified above.

292 **4. Numerical Experiments.** In this section, we detail the experiments conducted on a
293 small Electronic Health Records (EHR) dataset and discuss the results, showcasing a notable
294 increase in performance both in terms of overall accuracy and fairness metrics. For clarity
295 and to assist in interpreting the results, we include manifold projection plots generated using
296 Uniform Manifold Approximation and Projection (UMAP) [21]. The materials and code used
297 to generate these results are available in a repository¹.

298 **4.1. Dataset.** We performed our experiment on the Patient Treatment Classification
299 dataset², which comprises Electronic Health Records collected from a private hospital in
300 Indonesia. The dataset encompasses samples from 3309 patients; each sample consists of 8
301 scalar columns representing 8 kinds of continuous-valued laboratory blood test results and 2
302 binary variables, **SEX** and **SOURCE** which respectively represent our demographic and diagnosis
303 variables s and y .

304 Unlike most EHR datasets, this set was by default reasonably balanced, making it an
305 optimal choice for testing our methods. To ensure the dataset was exactly balanced at the
306 start of our experiment, we performed random undersampling such that each value of **SEX** was
307 represented equally. Since the dataset was already nearly balanced, this step only discarded a
308 handful of samples. We then generated a train/test split, where the train set serves as a “best-
309 case” control (referred to as the “original” set) and a test set provides an equitable set for our
310 experiments. Next, we deliberately created an imbalanced dataset by randomly drawing only
311 10% of samples from the minority class **F**, and 100% of samples from the majority class **M**.
312 After creating the imbalanced datasets, the set the was used to train the CDDPM contained
313 1792 samples.

314 DDPM models have historically exhibited optimal performance with high dimensional
315 datasets, such as those found in images, video, and sound. This dataset would normally
316 be considered poor for the application of such models due to its low dimensionality, limited
317 number of samples, and lack of translation or chirality invariances in our dataset when se-
318 lecting it. However, these same traits make the set a good adversarial test set for MCRAGE.

¹https://github.com/CalebFikes/MCRAGE-Emory_Math_REU_2023

²<https://www.kaggle.com/datasets/manishkc06/patient-treatment-classification>

319 Ultimately, our method showcased effectiveness even on this maladapted dataset, implying
320 potential success in a majority of real-world applications.

321 **4.2. Experimental Setup.** Our experiment consisted of two control and two treatment
322 groups. Our control groups are the original and imbalanced datasets. We applied MCRAGE
323 and SMOTE as our two treatment groups.

324 The more complex and time-consuming treatment was the MCRAGE group. In order to
325 tune the CDDPM model involved in MCRAGE, we first found a β -schedule which worked,
326 then fixed the diffusion time complexity T , and finally performed a grid search of 25 settings
327 for learning rate and dropout rate. We trained each model instance using the value $T' = 35$ for
328 10000 epochs, and saved the best checkpointed model. Every 100 epochs, we crossvalidated
329 the model by sampling the model according to MCRAGE and testing the performance of
330 a classifier trained on that set. In order to select a best model checkpoint, we selected the
331 diffusion model which generated the set that trained the classifier which achieved the highest
332 F1 score on a 10% validation split taken from the Imbalanced dataset. The best model was
333 reloaded and was used to generate synthetic minority data, which was then concatenated to
334 the original data according to the MCRAGE algorithm.

335 The SMOTE treatment group was simple, we applied SMOTE to the data, using labels
336 identical to s_0 in the MCRAGE algorithm. The SMOTE was significantly simpler and less
337 computationally expensive, but nonetheless offered a useful comparison for MCRAGE.

338 After each treatment dataset was created, it was used to train a Random Forest Classifier,
339 which was then tested on the test set. We report the resultant Accuracy, F1, and AUROC for
340 the classifier trained on data in each of the treatment groups. We have provided a flowchart
341 (Figure 1) for the readers convenience in understanding our setup.

342 **4.3. Sample Quality and Rebalancing Evaluation.** In order to verify that the generated
343 samples were meeting our expectations in terms of fidelity, we needed a method of easily
344 and subjectively assessing sample quality. For this purpose, we used UMAP to generate
345 manifold projections of our synthetic datasets and compared them to the original balanced and
346 artificially imbalanced sets [21]. Among the plots in Figure 2, it is evident that the MCRAGE
347 treated set is qualitatively more similar to the balanced set than the alternative SMOTE-
348 treated set. In our setting, where the primary concern is the performance of downstream
349 classifiers, the SMOTE method fails to generalize the trend of the minority data.

350 In particular, SMOTE is an inherently interpolation-based method, meaning that all sam-
351 ples generated by the technique are inside the convex hull of the original minority data. In
352 practice, when the minority group is sparse, SMOTE results in isolated clusters of minority
353 samples that do not have enough variance for a classifier trained on SMOTE-treated data to
354 adequately generalize many decision boundaries. This is detrimental to our goal of improv-
355 ing classifier performance, as the resultant minority samples must have sufficient variance for
356 the model to adequately learn a decision boundary that will perform well when diagnosing
357 individuals in the minority class.

358 As an empirical investigation of the theoretical convergence of CDDPMs, we sampled 4000
359 points from each class using our tuned CDDPM model and plotted the distributions against
360 the original data (Figure 3). The resulting histograms seem to indicate that the conditioned
361 samples are in fact converging to the conditional distribution represented in the data.

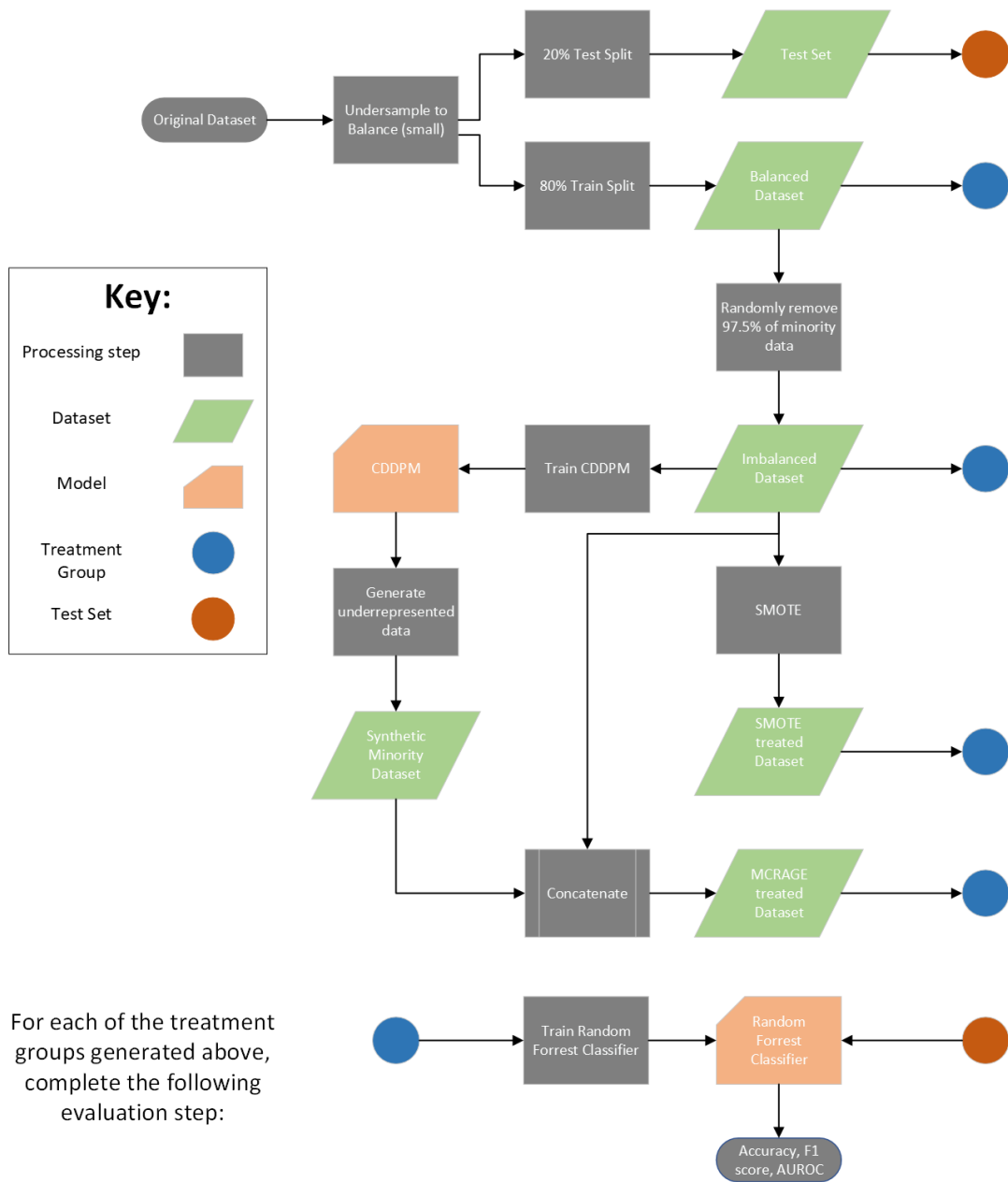


Figure 1: Flowchart detailing the experimental procedure

362 **4.4. Classifier Fairness Evaluation.** We will demonstrate the utility of our method with
 363 a binary classification task using a Random Forest classifier. For comparison to the current
 364 state-of-the-art, we also use SMOTE to rebalance the imbalanced dataset. Then, we evaluate
 365 the performance of the random forest classifier on each of the treated datasets and the balanced

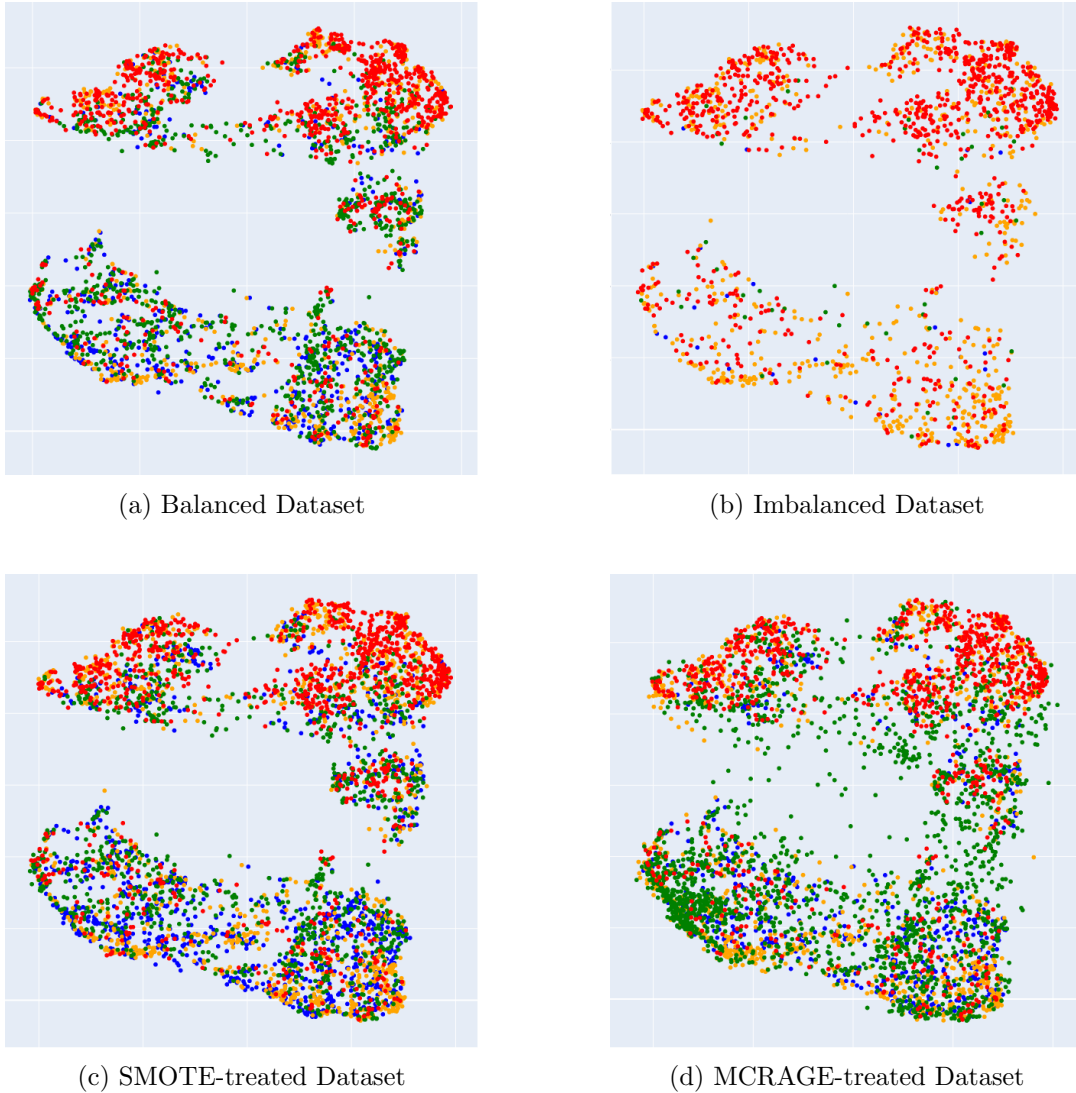


Figure 2: Manifold Projections of Classifier Training Datasets

366 and imbalanced control sets described previously. Resulting metrics are shown in the Table
 367 1. To evaluate the effectiveness of DDPM augmentation in improving downstream classifier
 368 fairness, we assess F1 score, which is the harmonic mean of precision and recall, because it
 369 considers both false positives and false negatives, making it more robust to class imbalances
 370 because it gives equal weight to both types of errors. In line with these assessments, we plotted
 371 kernel density estimation (KDE) plots, as shown in Figure 3, that compare the distributions
 372 of generated data against original data for selected features, to validate that our generated
 373 data distribution approximates the true distribution well.

374 Our method shows a clear improvement over both the imbalanced and SMOTE-treated

375 datasets. As seen in Table 1, the MCRAGE treated classifier shows a 4.69% increase in F1
 376 score over the imbalanced classifier, and a 4.42% increase over that of the SMOTE-treated
 377 classifier. As expected, the SMOTE-treated classifier shows a modest accuracy loss of 1.11%
 378 over the imbalanced control, whereas the MCRAGE treated one gained 1.59%. This poten-
 379 tially confirms our earlier observation that SMOTE tends to overfit, leading to potential losses
 380 in test performance. Surprisingly, the MCRAGE group classifier receives a 2.80% increase in
 381 F1 score versus the balanced control group. This defies conventional intuition because, treat-
 382 ing the MCRAGE process as one model, that model has a much worse training set than the
 383 balanced control set. However, the balanced control set is not *intersectionally* balanced, so the
 384 classifier trained on this set may still have discrepancies in performance between intersectional
 385 groups, leading to lower F1-score. Overall, the MCRAGE treated classifier exceeded expecta-
 386 tions in terms of F1 performance, demonstrating its novel utility as a dataset preprocessing
 387 step to promote fairness in downstream classifiers.

388 Moreover, as seen in Figure 3, for the features “MCHC” and “AGE”, our generated data
 389 distributions closely match the original distributions. This serves as motivation for future work
 390 in proving theoretical convergence results for conditioned diffusion models. This experiment
 391 verifies that the MCRAGE process can reliably increase the fairness of downstream classifiers
 392 relative to no treatment of demographic imbalance or SMOTE.

	Imbalanced	SMOTE	MCRAGE	Balanced
Accuracy (%)	71.348	70.555	72.480	73.160
F1 Score	0.64215	0.64384	0.67228	0.65396
AUROC	0.70	0.70	0.72	0.71

Table 1: Results of random forest classifier trained on different datasets.

393 **5. Discussion of Results.** The numerical experiment shows that MCRAGE treated data
 394 yields superior results in training fair downstream classifiers compared to the same process
 395 implemented with SMOTE treated or Imbalanced dataset. Our method yields significant
 396 improvement in accuracy, F1 score, and AUROC, where out of all the models only the balanced
 397 control classifier outperformed the MCRAGE treated one, and even then only in terms of raw
 398 accuracy. This demonstrates a novel application of the CDDPM architecture to promote
 399 fairness in healthcare or other consequential classification tasks.

400 In practice, most EHR datasets will perform like our imbalanced set due to intersectional
 401 imbalances, and the balanced set will be inaccessible. In situations where there is a signifi-
 402 cant class imbalance, it is beneficial to apply synthetic minority sampling techniques. There
 403 are cases where SMOTE may not be as effective, however: in datasets with sparse minor-
 404 ity groups, SMOTE-generated samples may exhibit a cluster-like behavior, so the synthetic
 405 samples generated by SMOTE may be concentrated in certain regions of the feature space,
 406 leading to potential losses in classification performance.

407 Implementing the MCRAGE process involves choosing an appropriate CDDPM architec-
 408 ture, tuning several hyperparameters, and often many training runs before achieving usable
 409 results. In practice, obtaining a model which can generate quality samples requires substan-

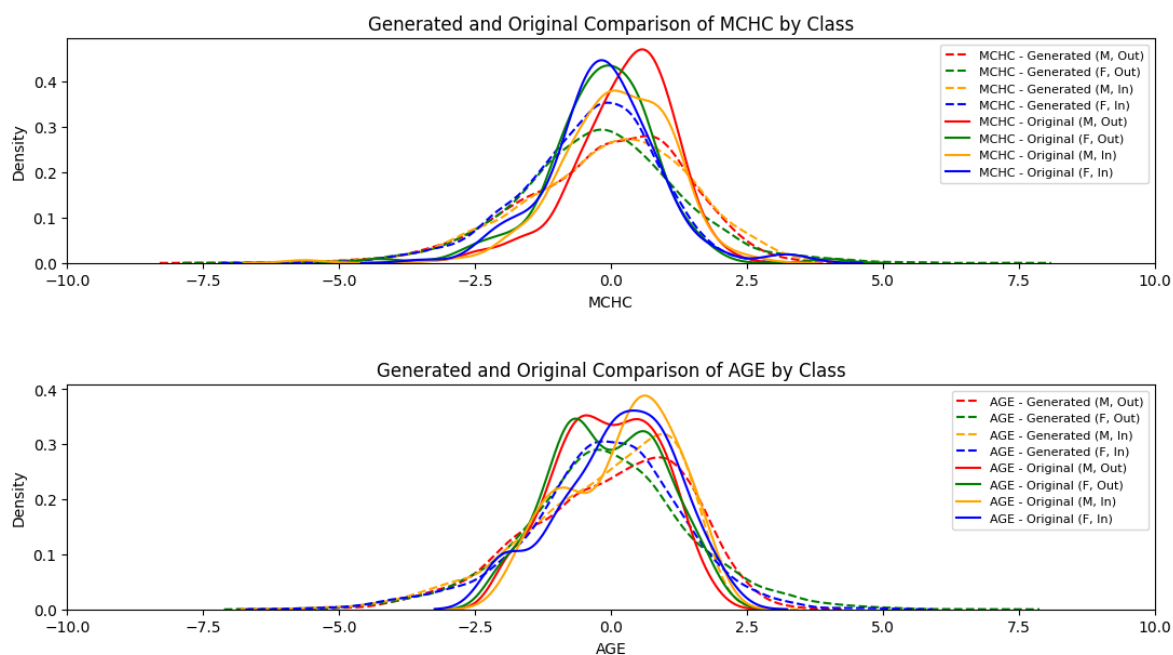


Figure 3: Conditional Sampling Distributions as compared to Data Distributions for 2 selected features of 9.

410 tial time, computational resources, and significant patience. By contrast, SMOTE is relatively
 411 simple and only has one parameter k , the number of neighbors to sample. We justify the differ-
 412 ence in implementation cost by the generality of application, broad evidence of performance,
 413 and explainability of fairness by way of the theoretical convergence guarantees stated above.
 414 In certain applications such as automated healthcare, benefits such as generality, performance,
 415 and explainability are simply worth this additional cost.

416 **6. Future Work and Limitations.** The MCRAGE algorithm, presented in this work, rep-
 417 represents a significant advancement in treating the pervasive issue of classifier bias stemming
 418 from demographic under-representation in training data. While this project has focused on
 419 applications to healthcare, similar methods could be applied to many other demographically-
 420 sensitive data; MCRAGE’s rigorous and versatile framework make it applicable across many
 421 fields.

422 To enhance the practicality and efficiency of MCRAGE, we propose a future approach
 423 that could further optimize the method’s performance. In practice, applying SMOTE to
 424 the data used to subsequently train a CDDPM seems to be the best strategy. By training the
 425 generative model on a dataset containing additional interpolated minority samples, the model
 426 is given more information and thus seems to obtain even better convergence for those classes.
 427 Although this method generated an exceptional F1 score, this method may not generalize as
 428 well, since the CDDPM will converge to a distribution which has been corrupted by SMOTE.

429 This approach offers a promising general-purpose fairness preprocessing step for demographic
430 disparity in data, and future testing may determine if it is as reliable as stock MCRAGE.

431 The field of generative modeling is characterized by dynamic advancements, and continu-
432 ous improvements in generative model architectures are expected to lead to more robust and
433 efficient results. Investigating similar architectures such as Mixtures of Experts of CDDPM,
434 CDDPM with different class guidance, conditional Poisson Flow Generative Models (PFGM)
435 [32] may deliver better samples and thus improve the performance of the process. These inno-
436 vations can offer more efficient and equally effective solutions, further establishing MCRAGE
437 as a pioneering approach in healthcare AI.

438 In conclusion, MCRAGE promises to mitigate data-induced classifier bias in healthcare
439 AI using a standardized framework for fairness-motivated synthetic data methods. By guar-
440 anteeing a best estimate of an equitable sample at relatively low cost, MCRAGE ensures
441 that equitable healthcare outcomes are available regardless of patient demographics or model
442 architecture.

443 **Acknowledgments.** This work is sponsored by NSF DMS 2051019. We would like to
444 thank Dr. Yuanzhe Xi for his mentorship during the REU program. We would also like to
445 acknowledge Huan He and Tianshi Xu for their collaboration and insight.

446

REFERENCES

- 447 [1] M. K. BAOWALY ET AL., *Synthesizing electronic health records using improved generative adversarial*
448 *networks*, Journal of the American Medical Informatics Association, 26 (2019), pp. 228–241, <https://doi.org/10.1093/jamia/ocy142>, <https://doi.org/10.1093/jamia/ocy142>.
- 449 [2] C. BELLINGER, R. CORIZZO, AND N. JAPKOWICZ, *Remix: Calibrated resampling for class imbalance in*
450 *deep learning*, 2020, <https://arxiv.org/abs/2012.02312>.
- 451 [3] V. BORTOLI, *Convergence of denoising diffusion models under the manifold hypothesis*, 2023.
- 452 [4] K. W. BOWYER, N. V. CHAWLA, L. O. HALL, AND W. P. KEGELMEYER, *SMOTE: synthetic mi-*
453 *nority over-sampling technique*, CoRR, abs/1106.1813 (2011), <http://arxiv.org/abs/1106.1813>, <https://arxiv.org/abs/1106.1813>.
- 454 [5] J. BUOLAMWINI AND T. GEBRU, *Gender shades: Intersectional accuracy disparities in commercial gen-*
455 *der classification*, in Proceedings of Machine Learning Research, vol. 81 of Conference on Fairness,
456 Accountability, and Transparency, 2018, pp. 1–15.
- 457 [6] Z. CHANG, G. A. KOULIERIS, AND H. P. H. SHUM, *On the design fundamentals of diffusion models: A*
458 *survey*, 2023, <https://arxiv.org/abs/2306.04542>.
- 459 [7] K. CHIN-CHEONG, T. SUTTER, AND J. E. VOGT, *Generation of heterogeneous synthetic electronic health*
460 *records using gans*, 2019-12-13, <https://doi.org/10.3929/ethz-b-000392473>. Workshop on Machine
461 Learning for Health (ML4H) at the 33rd Conference on Neural Information Processing Systems
462 (NeurIPS 2019); Conference Location: Vancouver, Canada; Conference Date: December 8-14, 2019.
- 463 [8] J. J. CHINN, I. K. MARTIN, AND N. REDMOND, *Health equity among black women in the*
464 *united states*, Journal of Women’s Health, 30 (2021), pp. 212–219, [https://doi.org/10.1089/jwh.](https://doi.org/10.1089/jwh.2020.8868)
465 2020.8868, <https://doi.org/10.1089/jwh.2020.8868>, <https://arxiv.org/abs/https://doi.org/10.1089/jwh.2020.8868>. PMID: 33237831.
- 466 [9] J. CHOI, S. KIM, Y. JEONG, Y. GWON, AND S. YOON, *ILVR: conditioning method for denoising diffusion*
467 *probabilistic models*, CoRR, abs/2108.02938 (2021), <https://arxiv.org/abs/2108.02938>, <https://arxiv.org/abs/2108.02938>.
- 468 [10] D. DABLAIN, B. KRAWCZYK, AND N. V. CHAWLA, *Deepsmote: Fusing deep learning and smote for*
469 *imbalanced data*, 2021, <https://arxiv.org/abs/2105.02340>.
- 470 [11] P. DHARIWAL AND A. NICHOL, *Diffusion models beat gans on image synthesis*, 2021, <https://arxiv.org/abs/2105.05233>.
- 471
- 472
- 473
- 474
- 475

- 476 [12] V. A. FAJARDO, D. FINDLAY, C. JAISWAL, X. YIN, R. HOUMANFAR, H. XIE, J. LIANG, X. SHE,
 477 AND D. EMERSON, *On oversampling imbalanced data with deep conditional generative models*, Expert
 478 Systems with Applications, 169 (2021), p. 114463, [https://doi.org/https://doi.org/10.1016/j.eswa.](https://doi.org/https://doi.org/10.1016/j.eswa.2020.114463)
 479 2020.114463, <https://www.sciencedirect.com/science/article/pii/S0957417420311155>.
- 480 [13] K. FUJIWARA, Y. HUANG, K. HORI, K. NISHIOJI, M. KOBAYASHI, M. KAMAGUCHI, AND M. KANO,
 481 *Over- and under-sampling approach for extremely imbalanced and small minority data problem in*
 482 *health record analysis*, Frontiers in Public Health, 8 (2020), p. 178, [https://doi.org/10.3389/fpubh.](https://doi.org/10.3389/fpubh.2020.00178)
 483 2020.00178.
- 484 [14] G. O. GHOSHEH, C. L. THWAITES, AND T. ZHU, *Synthesizing electronic health records for predictive*
 485 *models in low-middle-income countries (lmics)*, Biomedicine, 11 (2023), p. 1749, [https://doi.org/10.](https://doi.org/10.3390/biomedicine11061749)
 486 3390/biomedicine11061749, <http://dx.doi.org/10.3390/biomedicine11061749>.
- 487 [15] J. HENRICH, S. J. HEINE, AND A. NORENZAYAN, *The weirdest people in the world?*, Behavioral and Brain
 488 Sciences, 33 (2010), p. 61–83, <https://doi.org/10.1017/S0140525X0999152X>.
- 489 [16] J. HO, A. JAIN, AND P. ABBEEL, *Denoising diffusion probabilistic models*, CoRR, abs/2006.11239 (2020),
 490 <https://arxiv.org/abs/2006.11239>, <https://arxiv.org/abs/2006.11239>.
- 491 [17] J. HO AND T. SALIMANS, *Classifier-free diffusion guidance*, 2022, <https://arxiv.org/abs/2207.12598>.
- 492 [18] A. KOTELNIKOV, D. BARANCHUK, I. RUBACHEV, AND A. BABENKO, *Tabddpm: Modelling tabular data*
 493 *with diffusion models*, 2022, <https://arxiv.org/abs/2209.15421>.
- 494 [19] M. KOZIARSKI, *Radial-based undersampling for imbalanced data classification*, Pattern Recognition,
 495 102 (2020), p. 107262, <https://doi.org/https://doi.org/10.1016/j.patcog.2020.107262>, [https://www.](https://www.sciencedirect.com/science/article/pii/S0031320320300674)
 496 [sciencedirect.com/science/article/pii/S0031320320300674](https://www.sciencedirect.com/science/article/pii/S0031320320300674).
- 497 [20] S. H. LEE, *Natural language generation for electronic health records*, npj Digital Medicine, 1 (2018),
 498 <https://doi.org/10.1038/s41746-018-0070-0>, <https://doi.org/10.1038/s41746-018-0070-0>.
- 499 [21] L. MCINNES, J. HEALY, AND J. MELVILLE, *UMAP: Uniform manifold approximation and projection for*
 500 *dimension reduction*, 2020. Available online at [https://umap-learn.readthedocs.io/en/latest/index.](https://umap-learn.readthedocs.io/en/latest/index.html)
 501 [html](https://umap-learn.readthedocs.io/en/latest/index.html).
- 502 [22] S. MCLACHLAN., K. DUBE., T. GALLAGHER., B. DALEY., AND J. WALONOSKI., *The aten framework for*
 503 *creating the realistic synthetic electronic health record*, in Proceedings of the 11th International Joint
 504 Conference on Biomedical Engineering Systems and Technologies (BIOSTEC 2018) - HEALTHINF,
 505 INSTICC, SciTePress, 2018, pp. 220–230, <https://doi.org/10.5220/0006677602200230>.
- 506 [23] N. NORORI, Q. HU, F. M. AELLEN, F. D. FARACI, AND A. TZOVARA, *Addressing bias in big data and*
 507 *ai for health care: A call for open science*, Patterns, 2 (2021), p. 100347, [https://doi.org/10.1016/j.](https://doi.org/10.1016/j.patter.2021.100347)
 508 [patter.2021.100347](https://doi.org/10.1016/j.patter.2021.100347).
- 509 [24] N. NORORI, Q. HU, F. M. AELLEN, F. D. FARACI, AND A. TZOVARA, *Addressing bias in big data and*
 510 *ai for health care: A call for open science*, Patterns (N Y), 2 (2021), p. 100347, [https://doi.org/10.](https://doi.org/10.1016/j.patter.2021.100347)
 511 [1016/j.patter.2021.100347](https://doi.org/10.1016/j.patter.2021.100347).
- 512 [25] W. RAGHUPATHI AND V. RAGHUPATHI, *Big data analytics in healthcare: promise and potential*, Health
 513 Information Science and Systems, 2 (2014), <https://doi.org/10.1186/2047-2501-2-3>.
- 514 [26] A. RAJKOMAR, J. DEAN, AND I. KOHANE, *Machine learning in medicine*, New England Journal of
 515 Medicine, 380 (2019), pp. 1347–1358, <https://doi.org/10.1056/NEJMra1814259>.
- 516 [27] K. ROTH, A. LUCCHI, S. NOWOZIN, AND T. HOFMANN, *Stabilizing training of generative adversarial*
 517 *networks through regularization*, 2017, <https://arxiv.org/abs/1705.09367>.
- 518 [28] L. SEYYED-KALANTARI, H. ZHANG, M. B. A. MCDERMOTT, ET AL., *Underdiagnosis bias of artificial*
 519 *intelligence algorithms applied to chest radiographs in under-served patient populations*, Nature
 520 Medicine, 27 (2021), pp. 2176–2182, <https://doi.org/10.1038/s41591-021-01595-0>.
- 521 [29] Y. SONG AND S. ERMON, *Generative modeling by estimating gradients of the data distribution*, 2020,
 522 <https://arxiv.org/abs/1907.05600>.
- 523 [30] B. THEODOROU, C. XIAO, AND J. SUN, *Synthesize extremely high-dimensional longitudinal electronic*
 524 *health records via hierarchical autoregressive language model*, 2023, <https://arxiv.org/abs/2304.02169>.
- 525 [31] L. WANG, W. ZHANG, AND X. HE, *Continuous patient-centric sequence generation via sequentially coupled*
 526 *adversarial learning*, in Database Systems for Advanced Applications: 24th International Conference,
 527 DASFAA 2019, Chiang Mai, Thailand, April 22–25, 2019, Proceedings, Part II, Berlin, Heidelberg,
 528 2019, Springer-Verlag, p. 36–52, https://doi.org/10.1007/978-3-030-18579-4_3, [https://doi.org/10.](https://doi.org/10.1007/978-3-030-18579-4_3)
 529 [1007/978-3-030-18579-4_3](https://doi.org/10.1007/978-3-030-18579-4_3).

- 530 [32] Y. XU, Z. LIU, M. TEGMARK, AND T. JAAKKOLA, *Poisson flow generative models*, 2022, <https://arxiv.org/abs/2209.11178>.
531
532 [33] C. YAN, X. ZHANG, Y. YANG, AND ET AL., *Differences in health professionals' engagement with electronic*
533 *health records based on inpatient race and ethnicity*, *JAMA Netw Open*, 6 (2023), p. e2336383, <https://doi.org/10.1001/jamanetworkopen.2023.36383>.
534